Model based optimization of transflection near infrared spectroscopy as a process analytical tool in a continuous flash pasteurizer

Imke Weishaupt, Manuel Zimmer, Peter Neubauer, and Jan Schneider

Abstract: Near infrared spectroscopy in combination with a transflection probe was investigated as inline measurement in a continuous flash pasteurizer system with a sugar–water model solution. Robustness and reproducibility of fluctuations of recorded spectra as well as trueness of the chemometric analysis were compared under different process parameter settings. Variable parameters were the flow rate (from laminar flow at 30 L/h to turbulent flow at 90 L/h), temperature (20 to 100 °C) and the path length of the transflection probe (2 and 4 mm) while the pressure was kept constant at 2.5 bar. Temperature and path length were identified as the most affecting parameters, in case of homogenous test medium. In case of particle containing systems, the flow rate could have an impact as well. However, the application of a PLS model, which includes a broad temperature range, and the correction of prediction results by applying a polynomial regression function for prediction errors, was able to compensate these effects. Also, a path length of 2 mm leads to a higher accuracy. The applied strategy shows that by the identification of relevant process parameters and settings as well as the establishment of a compensation strategy, near infrared spectroscopy is a powerful process analytical tool for continuous flash pasteurization systems.

Keywords: flash pasteurization, inline near infrared spectroscopy, multivariate data analysis, process condition influences, sugar-water-solution model beverage

1. INTRODUCTION

Pasteurization is one of the most important steps in the beverage production as it does not only affect biological stability and the quality of the product, but also the energy expenditure. The pasteurization in a flash pasteurizer as a high temperature short time process (HTST) for example, is currently controlled only by the flow rate and the product outlet temperature and has therefore great potential for optimization. Using only the two parameters in the so called beer or fruit juice formula, the pasteurization units representing the lethal effect on microorganisms are determined. However, this calculation refers only to the holding section of the three-stage heat plate exchanger, not taking into account the heating and cooling section as well as the product specific properties. Despite the knowledge that it is a highly simplified model, it is still predominantly applied in the industry (Dammann, Schwarzer, Müller, & Schneider, 2011, 2014; Dammann, Schwarzer, Neubauer, & Schneider, 2014; Dammann, Schwarzer, Vullriede, Müller, & Schneider, 2012; Lewis & Heppell, 2012).

With an analytical tool that could be used to characterize both the product and the actual pasteurization effect, the entire process could be controlled in a more sustainable and product-friendly manner. In addition, the possibility of real-time quality control and a targeted process control as opposed to the current post-production-control would be enabled. So far, near infrared sensors, which are non-destructive and non-invasive, are promising to become a key technique in this field (Blanco & Romero, 2001; Debebe, Temesgen, Abshiro, & Chandravanshi, 2017; van den Berg, Lyndgaard, Sørensen, & Engelsen, 2013). The transfer from the chemical or, pharmaceutical sector to the food sector has been shown to be feasible on the basis of many studies (Bock & Connelly, 2008; Burns & Ciurczak, 2008; Cen & He, 2007; Grassi & Alamprese, 2018). Near infrared spectroscopy (NIRS) in combination with chemometric methods enables, for example, the determination of contents of certain ingredients, the classification of product groups, and the identification of provenances (Kessler, 2007; Porep, Kammerer, & Carle, 2015). In the sector of beverages, there have been many successful trials on wine, beer, fruit juices, and even on distilled alcoholic beverages (Cen, Bao, & He, Y. Sun, D.-W., 2007; Cozzolino, Cynkar, Shah, & Smith, 2011; Cozzolino, Parker, Dambergs, Herderich, & Gishen, 2006; Debebe et al., 2017; Gallignani, Garrigues, & de la Guardia, 1993; Halsey, 1985; Lachenmeier et al., 2010; Lanza & Li, 1984). However, food is usually a more complex system than chemicals or pharmaceuticals and processes are more unstable, which can make the implementation of NIRS difficult (Hitzmann et al., 2015; Osborne, 2006). Most of the existing studies do not take into account the problems that may occur with continuous inline measurements in industrial processes like in a heat treatment system for liquid foods (Porep et al., 2015).

There are only a few scientific studies dealing with non-constant measuring conditions such as fluctuating temperatures (Arimoto, Tarumi, & Yamada, 2003; Büning-Pfaue, 2003; Chen & Martin, 2007; Cozzolino et al., 2007; Golic, Walsh, & Lawson, 2003; Hageman, Westerhuis, & Smilde, 2017; Swierenga et al., 2000), showing that there are influences on NIR measurements. This makes it obvious that there is a need for further research on

JFDS-2019-1646 Submitted 10/7/2019, Accepted 4/29/2020. *Authors Weishaupt, Zimmer, and Schneider are with Department of Life Science Technologies, Institute of Food Technology.NRW, OWL University of Applied Sciences and Arts, Lemgo 32657, Germany (E-mail: imke.weishaupt@th-owl.de). Author Neubauer is with Bioprocess Engineering, Department of Biotechnology, Technische Universität Berlin, Berlin 13355, Germany. Direct inquiries to author Weishaupt (Email: imke.weishaupt@th-owl.de).*

doi: 10.1111/1750-3841.15307

Journal of Food Science A Publication of the Institute of Food Technologists

measuring conditions like the flow pattern (turbulent or viscosity dominated), pressure, or the high amount of water as main component in beverages, before NIRS can be implemented as PAT tool (Huang, Yu, Xu, & Ying, 2008). Hence, based on previous research results, this study follows the hypothesis that during inline process control in a flash pasteurizer, various influencing variables affect the NIRS measurement. It intends to explore process related influences on robustness, reproducibility, and accuracy of NIR measurements as well as to the process-analytical utilization of the measurement results by means of chemometric methods when analyzing a two-component system at the example of water–sugar-solutions in a flash pasteurization plant. Solutions have to be found to adjust these influencing variables before an implementation as PAT tool can be realized.

2. MATERIALS AND METHODS

Parameters had to be identified which impair the accuracy (consisting of the two criteria precision and trueness) of the NIRS measurement as inline PAT in an extend that is relevant for practical applications. Afterward, strategies for compensation of those impairments were undertaken. For identification of influencing parameters, the precision in terms of reproducibility was investigated, shown in the left work path of Figure 1. In a second work path the trueness was studied. Following the left work path, the reproducibility is derived from the comparison of measurements under the varying parameter settings of temperature and flow rate. With the tenfold measurement carried out for each parameter setting not only the reproducibility but also the repeatability and robustness has been determined. The variation coefficient (VC) has been used as a measure to express the precision (reproducibility) and was combined to a mean VC for all points of measurement (wavelengths) per spectrum.

The trueness (right path in Figure 1) was investigated by studying the effect of process conditions on the processing of spectra by applying chemometric methods and on the prediction performance (trueness). Therefore, the resulting models were compared regarding their performance. The workflow of modeling and the model performance key numbers are described in more detail below. After the evaluation of both criteria, precision and trueness, a correlation between these aspects was performed, leading to the evaluation of the accuracy.

2.1 Experimental setup and samples

NIR measurements were undertaken in an adapted laboratory heat treatment system for high temperature short time treatment type HT220 (OMVE, Utrecht, the Netherlands). The

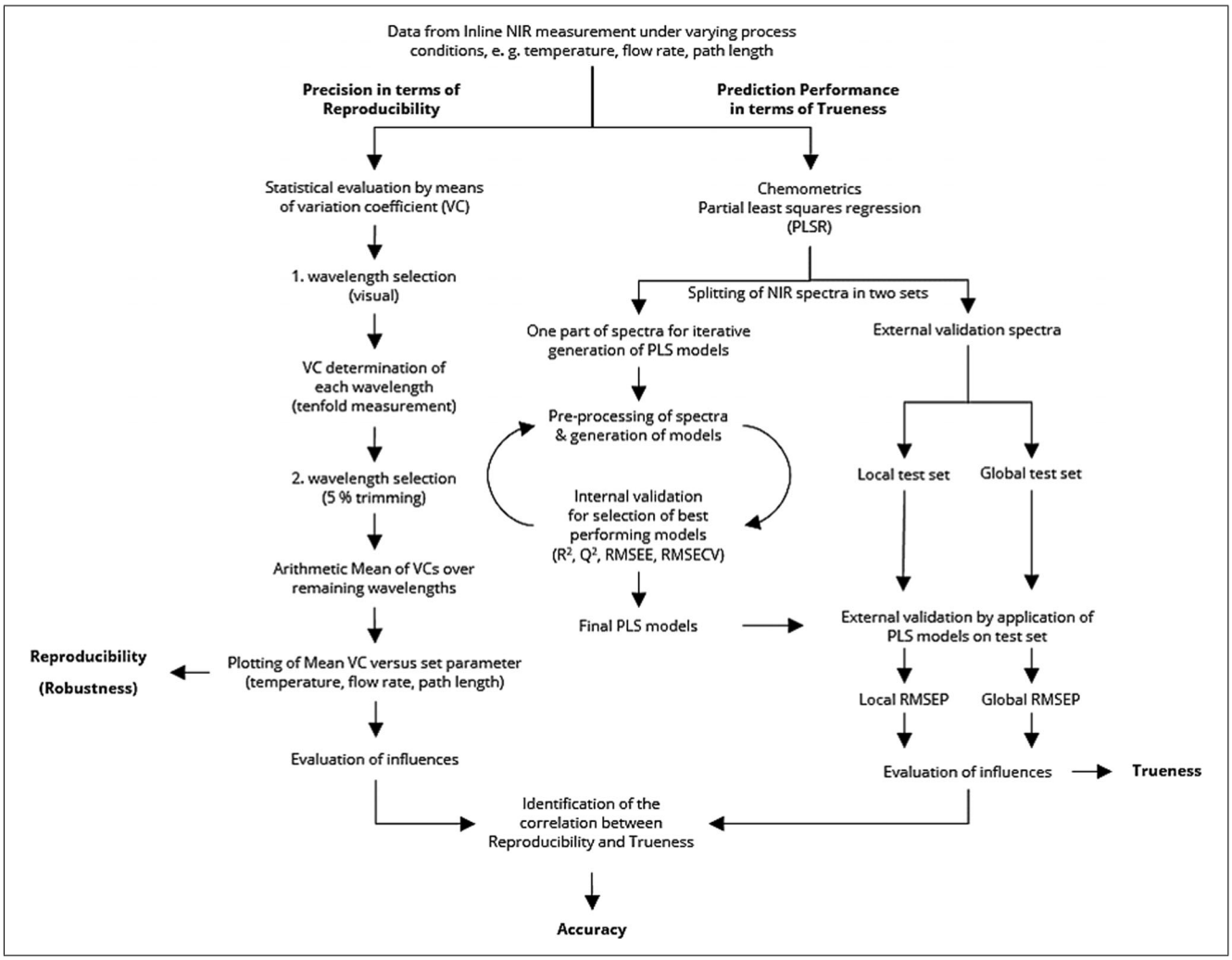

Figure 1–Workflow of the data analysis and evaluation: work path left evaluates the measurement preciseness and repeatability, work path right evaluates the effects on the spectra processing (abbreviations are described in section 2).

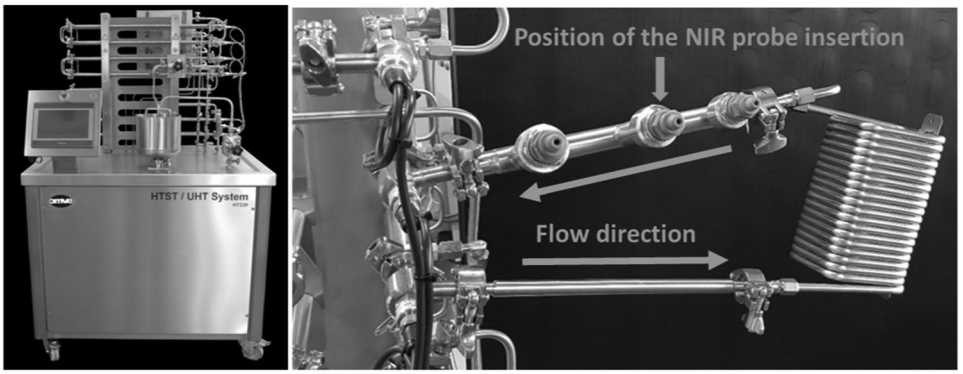

Figure 2–Adapted laboratory heat treatment system for high temperature short time treatment type HT220 (OMVE Netherlands B.V., 2018) (left) and extension with the holding tube coil and three connection options for implementation of measuring probes (right).

Table 1–Process parameters and settings in the experiments.

Temperature [°C]	Flow rate [L/h]	Sucrose concentration [g/L]
20	30	0
40	60	20
60	90	40
80		60
100		

Table 2–Reynold numbers for the different process settings in the tube diameter of 16 mm (laminar streaming condition Re < 2300; turbulent streaming condition Re > 2300 in italic).

		Reynolds number			
		Sugar concentration			
Temperature [°C]	Flow rate [L/h]	0 g/L	20 g/L	40 g/L	60 g/L
20	30	657	630	600	570
	60	1314	1259	1201	1140
	90	1972	1889	1801	1710
40	30	1005	961	916	870
	60	2009	1921	1831	1740
	90	*3014*	*2882*	*2747*	*2610*
60	30	1376	1321	1265	1208
	60	*2751*	*2642*	*2531*	*2417*
	90	*4127*	*3964*	*3796*	*3625*
80	30	1738	1682	1623	1561
	60	*3475*	*3363*	*3245*	*3121*
	90	*5213*	*5045*	*4868*	*4682*
100	30	2067	2019	1965	1905
	60	*4134*	*4038*	*3929*	*3809*
	90	*6200*	*6057*	*5894*	*5714*

temperature holding section was replaced by a tube coil (7 mm inner diameter, 0.269 L volume) and a short tube (16 mm inner diameter, 0.056 L volume) was implemented that served as measuring section with connection ports for various measuring probes like the transflection probe used for NIR measurement (Figure 2). According to Kümmel (2004), a stable flow pattern is ensured for all probe parts.

With this heat treatment system, different process parameter combinations, including a variation of temperature and flow rate, can be realized (shown in Table 1). The flow rate was adjusted to 30, 60, and 90 L/h, allowing for flow conditions from laminar to turbulent. The calculated Reynold numbers (Re) are shown in Table 2, where in a tube geometry Re < 2300 are considered to indicate laminar conditions and Re > 2300 turbulent conditions (Spurk, 1987). Five temperature levels (20, 40, 60, 80, and 100 °C) were taken into calculation of the Re using an empirical mathematical model according to Swindells, Snyder, Hardy, and Golden (1958) to calculate the kinematic viscosity of the used low-concentrated sugar solutions (Schmidt, 2000). Another process characteristic considered, the pressure (in a range of 2 to 4 bar), neither showed an effect on NIR spectra nor on the chemometric data analysis *(data not shown)*. Therefore, the pressure of the system was set constant at 2.5 bar for all experiments. Measured samples were water–sugar solutions in varying concentrations (0, 20, 40, and 60 g/L sucrose), which were prepared by dissolving crystalline sucrose in demineralized water.

2.2 Spectroscopic measurements

A PSS-2120 spectrometer (Polytec GmbH, Waldbronn, Germany) with a diode array of 256 pixels and a spectral range from 1100 to 2100 nm was used for inline NIR measurements. The spectrometer was combined with a transflection probe with variable path length (Avantes BV, Apeldoorn, the Netherlands), which was set at 2 or 4 mm. The Pas Labs 1.2 software (Polytec GmbH, Waldbronn, Germany) was taken to record spectra in absorbance mode with an integration time of 15 and 45 ms and an average of 100 measurements per spectrum. Demineralized water, tempered to 20 °C, was taken as reference medium. Reference spectra were measured in advance to the tenfold measurements that were recorded for each process parameter setting (Table 1).

2.3 Data analysis, spectral data pretreatment, and model generation

After recording the spectra, the two evaluation criteria (robustness and trueness) were examined, schematically illustrated in Figure 1. For data analysis in terms of precision (left path in Figure 1), raw spectral data were visualized in a first step to determine spectral "noise." The identified wavelength section between 1865 and 2100 nm was excluded from the evaluation as preprocessing step, reducing the original 256 wavelengths to 194 remaining signals. After trimming the 5% of highest values to prevent falsification and to make results more robust (Dialekt Projekt, 2002; Kähler, 2010), the arithmetic mean of the remaining 184 VCs was built for each parameter combination according to Table 1. The mean VCs, as a measure for the repeatability,

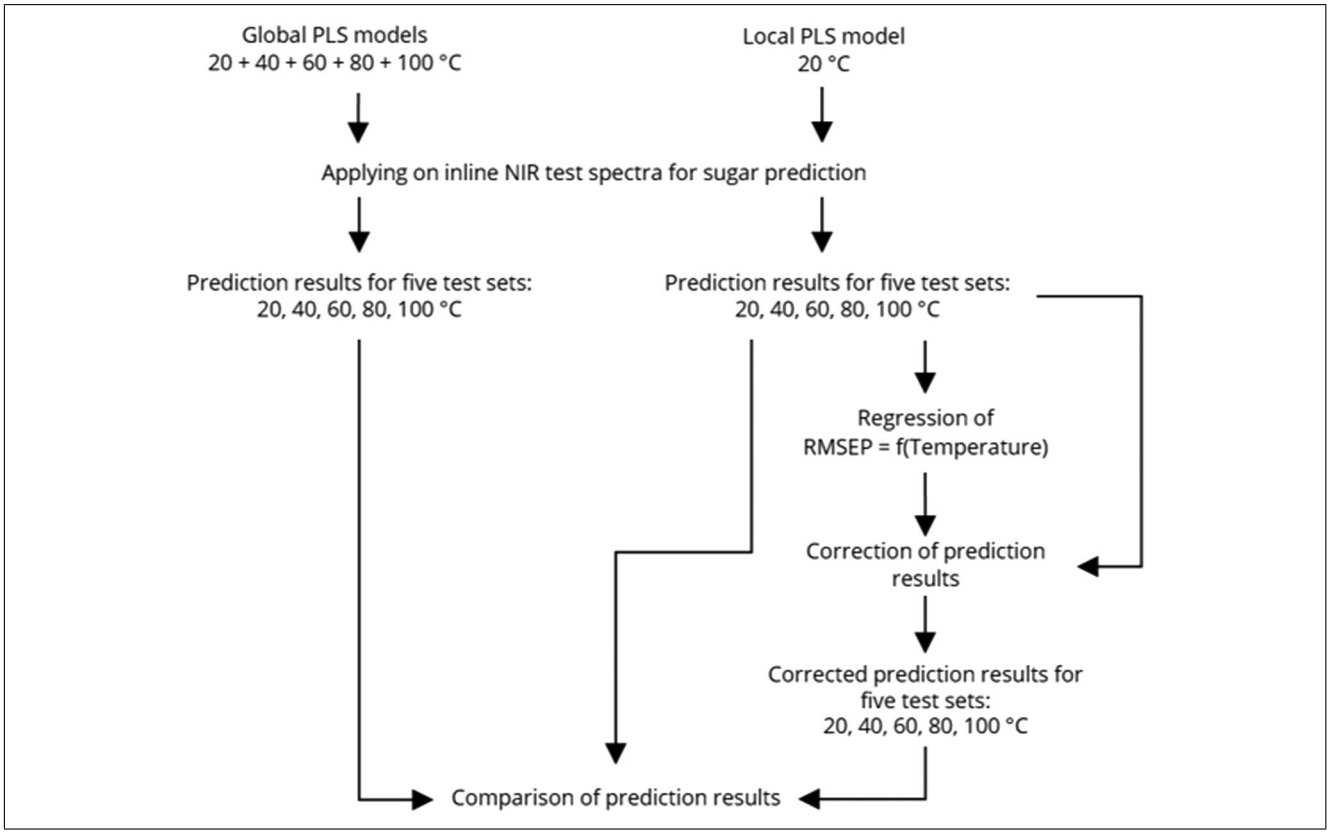

Figure 3–Schematic sequence of correction method development.

Table 3–Examination of the effect of the flow rate on the reproducibility; comparison of mean VC in % from a 10-measurement series for different levels of flow rate with 60 g/L sucrose at the five levels of temperature (CI with n = 184 and $\alpha = 0.05$).

	Temperature [°C]				
	20	40	60	80	100
			2 mm path length		
Flow rate [L/h]					
30	12.89 ± 1.67	5.03 ± 0.32	3.63 ± 0.11	1.15 ± 0.05	1.56 ± 0.05
60	5.24 ± 0.60	2.76 ± 0.17	3.24 ± 0.11	1.54 ± 0.06	2.38 ± 0.08
90	9.44 ± 0.98	7.65 ± 0.52	1.28 ± 0.04	0.77 ± 0.03	0.94 ± 0.07
			4 mm path length		
Flow rate [L/h]					
30	9.04 ± 0.96	6.04 ± 0.69	4.22 ± 0.55	2.54 ± 0.31	2.12 ± 0.24
60	5.16 ± 0.63	6.3 ± 0.66	4.39 ± 0.48	2.74 ± 0.38	2.33 ± 0.26
90	6.47 ± 0.70	8.28 ± 0.75	5.73 ± 0.56	1.28 ± 0.35	1.68 ± 0.33

were compared among the factor combinations temperature and flow rate. The statistical indicator VC was chosen to make the results of different path lengths of the probe comparable (Adams, 2004). The conclusions of the VC comparison were examined for statistical significance using an ANOVA analysis and *t*-tests for value classification.

For chemometric analysis (right path in Figure 1), Simca 14.1 (MKS Umetrics AB, Malmö, Sweden) was used. Five spectra of the 10-fold measurement were used as a training set and the other five as an internal validation set. For modeling, the different levels of the parameters result in data sets of varying size depending on the reference parameter that is kept constant. The models for each level of temperature were based on 100 spectra, models regarding the parameter of flow rate included 60 spectra. Regression models were made by using the PLS regression method in an iterative process applying different preprocessing methods to optimize the model quality. Savitzky–Golay smoothing and Standard Normal Variate transformation (SNV) as well as Multi Scatter Correction (MSC) smoothing techniques were applied. Furthermore, the first and second derivations were formed and proved for an improvement on model quality.

For evaluation, the coefficient of determination (R^2) and the predictive quality (Q^2) as well as the two parameters root mean square error of estimation (RMSEE) and the root mean square error of cross-validation (RMSECV) were determined using Simca. R^2 is a measure of the variance of the total variance explained by the model. Q^2 is a measure for the predictive ability and results from the internal cross-validation. Both should have values close to the maximum value of 1. The latter two parameters are a common measure in statistics to allow an evaluation of the scatter of the prognosis values with low values indicating a high model quality. To avoid overfitting, a permutation-test was applied, which

Table 4–Two-factorial ANOVA analysis for the parameters temperature and flow rate (2 and 4 mm path length).

	Factor	*F*	*p*-Value	*F crit*	Interpretation
			2 mm path length		
Sugar concentration [g/L]					
0	Flow rate	2.990	0.107	4.459	No significant effect
	Temperature	*18.705*	*0.0004*	3.838	*p*-Value smaller than .05, significant effect
20	Flow rate	1.799	0.226	4.459	No significant effect
	Temperature	27.563	9.90706×10^{-05}	3.838	*p*-Value smaller than .05, significant effect
40	Flow rate	0.216	0.810	4.459	No significant effect
	Temperature	18.914	0.0004	3.838	*p*-Value smaller than .05, significant effect
60	Flow rate	0.336	0.724	4.459	No significant effect
	Temperature	10.874	0.003	3.838	*p*-Value smaller than .05, significant effect
			4 mm path length		
Sugar concentration [g/L]					
0	Flow rate	0.972	0.419	4.459	No significant effect
	Temperature	*6.594*	*0.012*	3.838	*p*-Value smaller than .05, significant effect
20	Flow rate	1.217	0.346	4.459	No significant effect
	Temperature	2.500	0.126	3.838	No significant effect
40	Flow rate	0.539	0.603	4.459	No significant effect
	Temperature	*9.054*	*0.005*	3.838	*p*-Value smaller than .05, significant effect
60	Flow rate	0.670	0.538	4.459	No significant effect
	Temperature	*6.667*	*0.012*	3.838	*p*-Value smaller than .05, significant effect

Table 5–Results of *t*-test and conclusions regarding a correlation between the level of flow rate and the mean CV; including both path length; with *t crit* 1.65.

path length	Compared levels	mean CVs	*t stat*	*p*-Value	Conclusion
Example 1: parameter setting 40 g/L and 80 °C					
2 mm	30 | 60 L/h	1.14 | 2.05	−14.181	2.1759×10^{-35}	CV(30)<CV(60)>CV(90)
	60 | 90 L/h	2.05 | 1.19	23.534	3.6538×10^{-69}	
4 mm	30 | 60 L/h	2.19 | 2.95	−3.426	0.00034645	CV(30)<CV(60)>CV(90)
	60 | 90 L/h	2.95 | 1.91	5.654	1.58991×10^{-08}	
Example 2: parameter setting 60 g/L and 100 °C					
2 mm	30 | 60 L/h	0.94 | 2.38	18.028	3.5447×10^{-50}	CV(30)>CV(60)<CV(90)
	60 | 90 L/h	2.38 | 1.56	−27.531	4.2204×10^{-91}	
4 mm	30 | 60 L/h	2.12 | 2.33	−1.180	0.11946419	CV(30)≈CV(60)>CV(90)
	60 | 90 L/h	2.33 | 1.68	3.028	0.00132277	
Example 3: parameter setting 20 g/L and 40 °C					
2 mm	30 | 60 L/h	4.88 | 2.72	16.681	1.2263×10^{-43}	CV(30)>CV(60)<CV(90)
	60 | 90 L/h	2.72 | 5.44	−26.164	1.3811×10^{-81}	
4 mm	30 | 60 L/h	6.52 | 7.86	−4.291	1.15811×10^{-05}	CV(30)<CV(60)>CV(90)
	60 | 90 L/h	7.86 | 6.10	5.171	2.05791×10^{-07}	

serves for controlling the statistical significance of the model and its ability to predict unknown samples.

In order to determine possible influences by the process parameters, temperature, and flow rate, individual models were generated for each set level, which have the same configurations to make them comparable. This type of PLS model, which includes only one adjusted level of process parameter, is called local model. Therefore, there were five models, one for each level of temperature and three for flow rate, respectively.

After model fitting, an external validation with the second part of the recorded spectra was performed. This resulted in the RMSEP as quality parameter, which was calculated using local and global test sets. Local in this case means that spectra based on the same process conditions of the calibration spectra were used. Global test sets, on the other hand, contain all process parameter ranges. The comparison enabled the identification of possible correlations between prediction quality and process parameters and thus in the end possible influencing parameters. All these investigations were done for both path lengths to verify whether there is a dependence on the path length of the probe. Finally, interactions between reproducibility and trueness were investigated and conclusions were made about the accuracy.

2.4 Correction of parameters with regard to the prediction of sugar concentration

Two types of PLS models were examined to compensate for temperature induced deviations, namely global PLS models with all five temperature levels and a local PLS model based on spectra recorded at 20 °C. Both procedures were based on spectra recorded with the path length of 2 mm shown schematically in Figure 3.

For the global PLS models, the iterative procedure of fitting described in the previous section was repeated. In total two global PLS models were generated: one for direct comparison with the local model and one in terms of optimized prediction performance. These two global models as well as the local model were applied to the five local test sets (20, 40, 60, 80, and 100 °C) to predict the sugar concentration and determine the RMSEP values. Using the RMSEP values of local model a polynomial regression was carried out and the statistical evaluation was performed by

Table 6–Comparison of model quality for different flow rate built from the spectra of the path length of 2 and 4 mm.

Flow rate [L/h]	LV	N	R^2_X	R^2_Y	Q^2	RMSEE	RMSECV
			Path length of 2 mm				
30	5	100	1	1	1	0.358	0.697
60	5	100	1	1	1	0.448	0.500
90	5	100	1	1	1	0.444	0.498
			Path length of 4 mm				
30	5	100	1	0.996	0.996	1.404	1.476
60	5	100	1	0.996	0.995	1.517	1.572
90	5	100	1	0.998	0.998	0.934	1.000

Abbreviations: LV, number of latent variables; N, number of spectra included in calibration set

Table 7–RMSEPs of a local test set (based on flow rate of calibration set) and a global test set (based on all flow rate levels).

	2 mm Path length		4 mm Path length	
	Local	Global	Local	Global
Flow rate [L/h]				
30	0.383	0.388	1.928	1.577
60	0.421	0.415	1.538	1.538
90	0.366	0.401	0.879	1.292

an ANOVA analysis and a *t*-test for the regression coefficients. With the resulting regression equation as a function of measuring temperature, the sugar concentration of the several test sets, which were predicted by applying the local model, were adjusted. Finally, prediction performance of the three models was compared.

3. RESULTS AND DISCUSSION

3.1 Effect of flow rate and current pattern on robustness and repeatability of NIR measurements

NIR spectra were investigated for their repeatability and robustness at different flow rates or rather current pattern and two different path lengths. The VC of a 10-fold measurement and the 5% confidence interval (CI) were used as a measure (results are shown in Table 3). The results for the VC vary unsystematically regarding the level of the flow rate. Since no correlation between flow rate level or rather the current pattern and the mean VC can be seen for both path lengths, the flow rate seems to have no identifiable effect on the robustness and repeatability of measurement. Solely the stabilizing effect of a smaller path length could be proven by means of a narrower 5% CI. By means of a statistical evaluation, these statements were checked and proven at a significance level of 5%. By applying the two-factorial ANOVA analysis (with the factors temperature and flow rate), no effect of the flow rate could be identified (Table 4). The one-factorial ANOVA analysis showed significant differences for the mean CVs, which could not be systematically correlated with the level of the flow rate by applying the *t*-test (results are shown Table 5).

3.2 Effect of flow rate and current pattern on chemometric analysis of NIR measurements

Influences of flow rate on NIR data analysis were investigated regarding the quality of sugar concentration prediction by fitting PLS models. Using the raw spectra of both path lengths, a wavelength exclusion from 1401 to 1517 nm and from 1865 to 2100 nm was carried out. Information and quality parameters of the fitted PLS models are given in Table 6. By determining the RMSEPs for local and global test sets, influences of the flow rate were investigated. The results, given in Table 7, showed no difference between local and global test sets and there were only slight differences between the levels of flow rates. In comparison of the two path length, the RMSEP values of the 2 mm one were about a third. This is also represented in the ratio of the RMSEPs to the average quantity of sugar (30 g/L), where the percentile values of a path length of 2 mm differ between 1.22% and 1.40% and of the larger path length between 2.93% and 6.43%. In conclusion, taking into account that a smaller path length leads to a higher reproducibility and that the results for local and global test sets show comparable behavior, the flow condition seems to have no relevant impact on the trueness of the analyte determination. This could already be guessed by looking at the raw spectra, colored by the level of flow rate in Figure 4. No systematic differentiation between the three levels of flow rate can be examined. One theory supporting this assumption could be that water–sugar solutions are homogeneous mixtures in which the exchange between the different flow planes is not improved or worsened by higher turbulence compared with purely parallel velocity vectors (laminar). Therefore, the effect could be different for an inhomogeneous medium that contains particles.

3.3 Effect of temperature on robustness and repeatability of NIR measurements

The effect of measuring temperature on robustness and repeatability was established by calculating the VC of a 10-fold measurement in comparison of two path lengths. Besides this, the 5% CI was calculated as a measure. As can be seen in Table 8, the mean VCs and the CIs have the highest values at 20 °C. In addition to the height of the absolute values, the range of the values is also largest here. As the measuring temperature increases, there is a trend toward decreasing VC values and also the CIs become narrower. This trend can be observed for both path lengths, whereby the values of the path length of 2 mm are generally smaller (only measurements at 20 °C showed deviations from this trend). This demonstrate a positive impact of higher temperatures and of a smaller path length on robustness and reproducibility. These statements, which were obtained by comparing the mean CV and the CI, could be statistically confirmed as significant at a significance level of 5%. The two-factorial ANOVA analysis showed a significant effect for temperature (Table 4). By applying the *t*-test, the values of the mean CV could be classified in the systematic (inverse) correlation with the temperature level. Results of statistical evaluation are summarized in Table 9.

3.4 Effect of temperature on chemometric analysis of NIR measurements

For evaluation of temperature influence on sugar prediction, comparable PLS models were generated by using raw spectra and

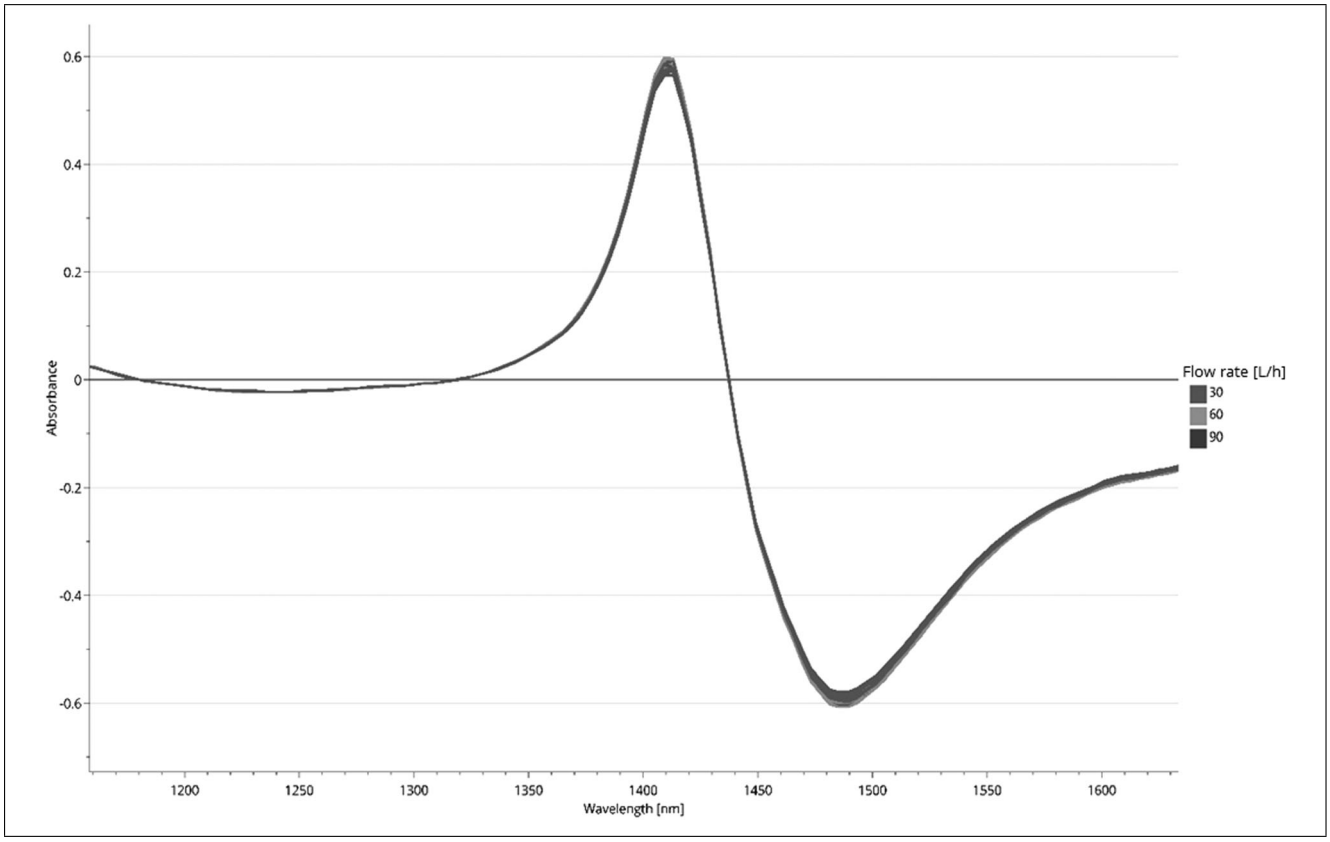

Figure 4–Raw spectra measured at 80 °C with 60 g/L sucrose colored by level of flow rate with in the wavelength range between 1100 and 1650 nm.

Table 8–Examination of the effect of the temperature on the reproducibility; comparison of mean VC from a 10-measurement series for different levels of temperature with 60 g/L sucrose and the flow rate of 30, 60, and 90 L/h; confidence intervals with $n = 184$ and $\alpha = 0.05$.

		Temperature [°C]				
Flow rate	**Path length**	**20**	**40**	**60**	**80**	**100**
30 L/h	2 mm	12.89 ± 1.67	5.03 ± 0.32	3.63 ± 0.11	1.15 ± 0.05	1.56 ± 0.05
	4 mm	9.04 ± 0.96	6.04 ± 0.69	4.22 ± 0.55	2.54 ± 0.31	2.12 ± 0.24
60 L/h	2 mm	5.24 ± 0.6	2.76 ± 0.17	3.24 ± 0.11	1.54 ± 0.06	2.38 ± 0.08
	4 mm	5.16 ± 0.62	6.3 ± 0.66	4.39 ± 0.48	2.74 ± 0.38	2.33 ± 0.26
90 L/h	2 mm	9.44 ± 0.98	7.57 ± 0.5	1.28 ± 0.04	0.77 ± 0.03	0.94 ± 0.07
	4 mm	6.47 ± 0.7	8.28 ± 0.75	5.73 ± 0.56	1.28 ± 0.35	1.68 ± 0.33

excluding the wavelengths from 1401 to 1517 nm and from 1865 to 2100 nm. The RMSEPs for a local and a global test set were calculated and compared for evaluation. Relevant information about the number of spectra included in the calibration set, the number of LVs of the model, and also the quality parameters are summarized in Table 10. RMSEPs of local test set showed increasing behavior with higher temperatures, RMSEPs of global test sets had lowest values with the mean measuring temperature of 60 °C and increased to the edges of the examination range. This is illustrated in Table 11. Also shown is that RMSEPs of global test sets had their maximum value in the range of maximum concentration of sugar (60 g/L), while RMSEPs of local test sets were much lower. The ratio to the mean sugar concentration (30 g/L) of local test sets is between 0.22% and 3.52%, of the global test sets between 53.54% and 190.95%. In case of local test sets the smaller path length shows lower prediction errors. The different behavior and higher values of RMSEP of local and global test set showed an impact of the temperature on the trueness of prediction results. Lower temperatures for modeling generated more variance in PLS model and this led to better prediction results. Furthermore, the results of RMSEPs for global test set show a different behavior than for local test set. The direct influence of temperature on the shape of the spectra and thus on the chemometric analysis could also be shown on the basis of the raw spectra. By coloring according to the temperature, an increase in absorption could be shown with increasing temperature (shown in Figure 5).

3.5 Integration of temperature influence on prediction results by global modeling

As the temperature has been revealed of being a relevant influencing parameter, the approach of fitting global PLS models has been pursued for its compensation. This was done by

Table 9–Results of t-test and conclusions regarding a correlation between the level of temperature and the mean CV; including both path length; with *t crit* 1.65.

Path length	Compared levels	mean CVs	*t stat*	*p*-Value	Conclusion
Example 1: parameter setting 40 g/L and 90 L/h					
2 mm	20 | 40 °C	7.99 | 2.41	8.667	7.1271×10^{-17}	CV(20)>CV(40)>CV(60)>CV(80)>CV(100)
	40 | 60 °C	2.41 | 1.39	2.217	0.0139266	
	60 | 80 °C	1.39 | 1.19	6.488	1.62×10^{-10}	
	80 | 100 °C	1.19 | 1.02	6.174	9.0221×10^{-10}	
4 mm	20 | 40 °C	7.56 | 7.56	-0.006	0.497729598	CV(20)≈CV(40)>CV(60)>CV(80)>CV(100)
	40 | 60 °C	7.56 | 3.33	13.737	7.07445×10^{-35}	
	60 | 80 °C	3.33 | 1.91	6.065	1.79859×10^{-09}	
	80 | 100 °C	1.91 | 1.06	5.003	4.56273×10^{-07}	
Example 2: parameter setting 60 g/L and 30 L/h					
2 mm	20 | 40 °C	12.89 | 5.03	9.047	7.0735×10^{-17}	CV(20)>CV(40)>CV(60)>CV(100)
	40 | 60 °C	5.03 | 3.63	8.045	2.5424×10^{-14}	
	60 | 80 °C	3.63 | 1.15	41.463	7.427×10^{-115}	
	80 | 100 °C	1.15 | 1.56	-12.168	3.8682×10^{-29}	
	60 | 100°C	3.63 | 1.56	34.705	1.1244×10^{-97}	
4 mm	20 | 40 °C	9.04 | 6.04	4.987	4.95506×10^{-07}	CV(20)>CV(40)>CV(60)>CV(80)>CV(100)
	40 | 60 °C	6.04 | 4.22	4.053	3.11906×10^{-05}	
	60 | 80 °C	4.22 | 2.54	5.239	1.56262×10^{-07}	
	80 | 100 °C	2.54 | 2.12	2.107	0.017925001	
Example 3: parameter setting 40 g/L and 30 L/h					
2 mm	20 | 40 °C	11.10 | 3.94	10.767	8.5235×10^{-22}	CV(20)>CV(40)>CV(60)>CV(80)≈CV(100)
	40 | 60 °C	3.94 | 1.91	16.788	1.2615×10^{-41}	
	60 | 80 °C	1.91 | 1.14	11.456	5.5609×10^{-26}	
	80 | 100 °C	1.14 | 1.12	0.271	0.393	
4 mm	20 | 40 °C	9.14 | 4.52	8.939	2.09542×10^{-17}	CV(20)>CV(40)>CV(60)>CV(80)>CV(100)
	40 | 60 °C	4.52 | 3.15	4.381	8.23381×10^{-06}	
	60 | 80 °C	3.15 | 2.19	3.974	4.27231×10^{-05}	
	80 | 100 °C	2.19 | 1.48	3.498	0.000274712	

Table 10–Comparison of model quality for different temperatures built from the spectra of the path length of 2 and 4 mm.

Temperature [°C]	LV	*N*	R^2_X	R^2_Y	Q^2	RMSEE	RMSECV
			Path length of 2 mm				
20	4	60	0.999	1	1	0.076	0.302
40	4	60	1	1	1	0.101	0.657
60	4	60	1	1	1	0.076	0.463
80	4	60	1	1	1	0.143	0.502
100	4	60	1	1	1	0.165	1.070
			Path length of 4 mm				
20	4	60	0.997	0.999	0.999	0.544	0.579
40	4	60	0.998	0.999	0.999	0.579	0.648
60	4	60	0.998	1	1	0.332	0.716
80	4	60	0.998	1	0.999	0.530	0.643
100	4	60	0.994	0.998	0.998	0.911	1.012

Abbreviations: LV, number of latent variables; *N*, number of spectra included in calibration set.

Table 11–RMSEP values for local test set and global test set in grams per liter, resulting from measurements with the two path lengths of 2 and 4 mm; local test set based on temperature of calibration set; global test set based on all temperature levels.

	2 mm path length		4 mm path length	
Temperature [°C]	Local	Global	Local	Global
20	0.067	0.537	57.286	46.104
40	0.081	0.57	29.06	21.402
60	0.1	0.41	20.086	16.063
80	0.136	0.74	35.153	26.295
100	0.16	1.056	54.155	49.6

including a broad range of temperatures in the calibration set of spectra, like Arimoto et al. (2003) applied in their study about an temperature-insensitive PLS model to predict glucose concentration. Two global PLS models were fitted: one with the same number of LVs for a direct comparison of results of local and global model, one with a higher number of LVs in terms of optimized model performance. The preprocessing was done analogous to the generation of local PLS model to make it comparable. Details about the number of spectra included in the calibration set, the number of LVs of the model as well as the quality parameters are summarized in Table 12. The properties of the local model

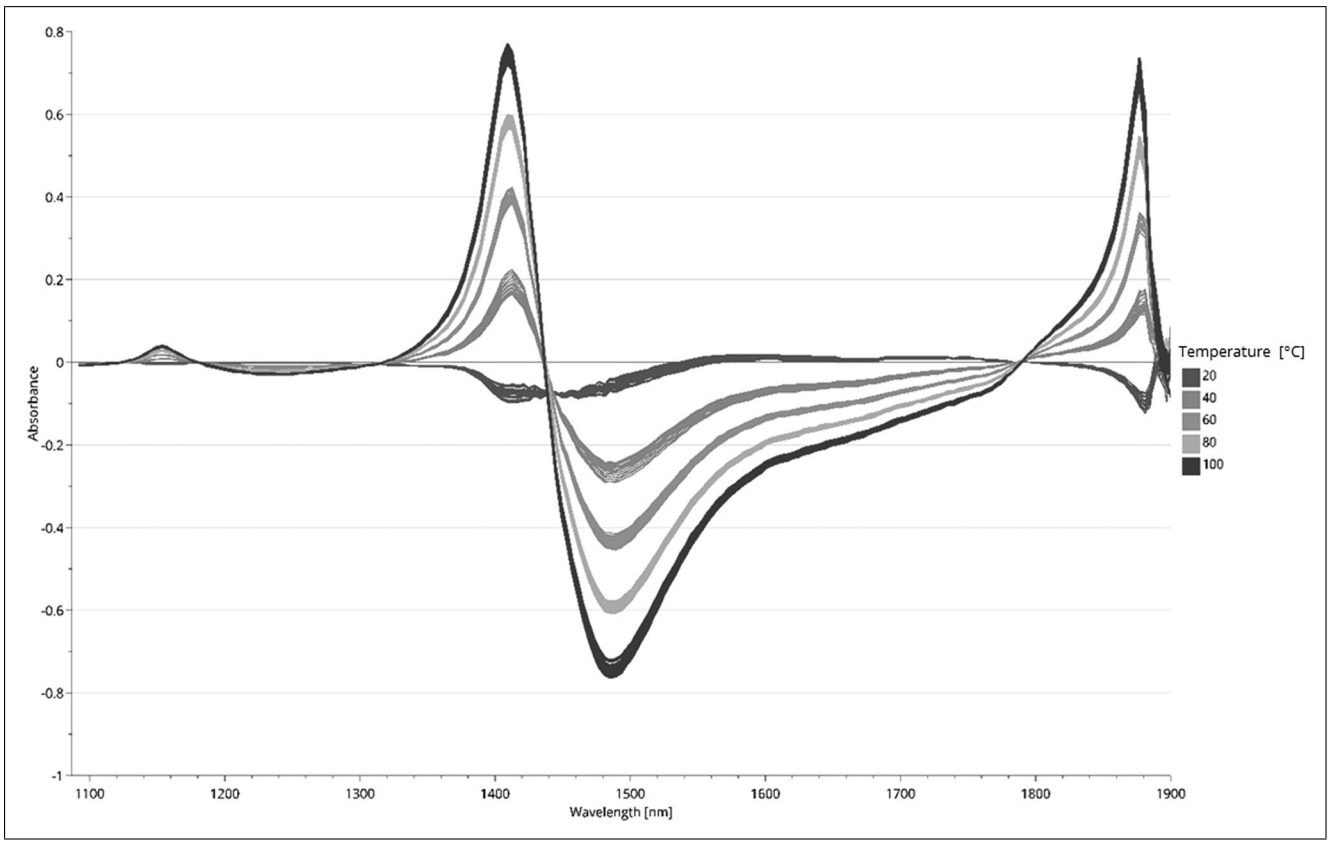

Figure 5–Raw spectra measured at five different stages of temperature with 60 g/L sucrose colored by level of temperature with in the wavelength range between 1100 and 1900 nm.

Table 12–Information about model properties used for temperature compensation strategies.

Model type	LV	*N*	R^2_X	R^2_Y	Q^2	RMSEE	RMSECV
Local (20 °C)	4	60	0.999	1	1	0.076	0.302
Global (direct comparison)	4	60	1	0.995	0.995	1.776	2.109
Global (high performance)	5	60	1	1	1	0.460	2.750

Table 13–Results of RMSEP as a measure for prediction quality for the sugar concentration by applying different types of PLS models on test sets of different measuring temperatures; RMSEP values in g/L.

	Calculated with		
	Local model	Global model (direct comparison)	Global model (performance optimized)
Temperature [°C] of test set			
20	0.067	1.841	0.258
40	9.048	1.442	0.482
60	31.706	1.171	0.221
80	64.647	1.148	0.53
100	105.72	1.992	0.441

based on 20 °C spectra are also listed there. RMSEPs were focused for evaluation of prediction quality. Results of both global models were stable over the different temperature stages, whereas RMSEP of local model increased with distance to the measuring temperature as can be seen in Table 13. The global model for comparison showed a percentage error between 3.83% and 6.64% in relation to the mean sugar quantity, the optimized model only between 0.74% and 1.77%. Thus, local models prove to be suitable only in the range of their calibration temperature, whereas global models have acceptable error levels and are universally applicable.

3.6 Integration of temperature influence on prediction results by polynomial regression

Another approach to compensate the influence of temperature was the subsequent correction of the prediction results reached with the local model by calculating a regression equation for the growth of the RMSEP as a function of the temperature. By using the RMSEP values given in Table 13 (results of local model), the numerical value equation $\text{RMSEP} = -5.603 \times 10^{-05}\ T^3 + 0.0235\ T^2 - 0.8086\ T + 7.2834$ resulted with a coefficient of determination R^2 of 1. The dimensions here are in grams per

Table 14–Regression Statistics for polynomial regression.

Multiple *R*	**0.99999953**
R^2	**0.99999906**
Adjusted R^2	**0.99999622**
Standard Error	**0.08428752**
Observation	**5**

ANOVA

	df	*SS*	*MS*	*F*	*Significance F*
Regression	3	7527.42217	2509.14072	353181.911	0.00123694
Residual	1	0.00710439	0.00710439		
Total	4	7527.42927			

t-Test	Coefficients	Standard Error	*t Stat*	*p*-Value	Lower 95%	Upper 95%
Intercept	7.28336	0.41463978	17.5655119	0.03620352	2.01486205	12.551858
T	−0.8085805	0.02709985	−29.837084	0.02132854	−1.1529167	−0.4642442
T^2	0.02353339	0.00050293	46.792896	0.01360298	0.0171431	0.02992368
T^3	-5.603×10^{-05}	2.7765×10^{-05}	-20.180044	0.03152121	-9.131×10^{-05}	-2.075×10^{-05}

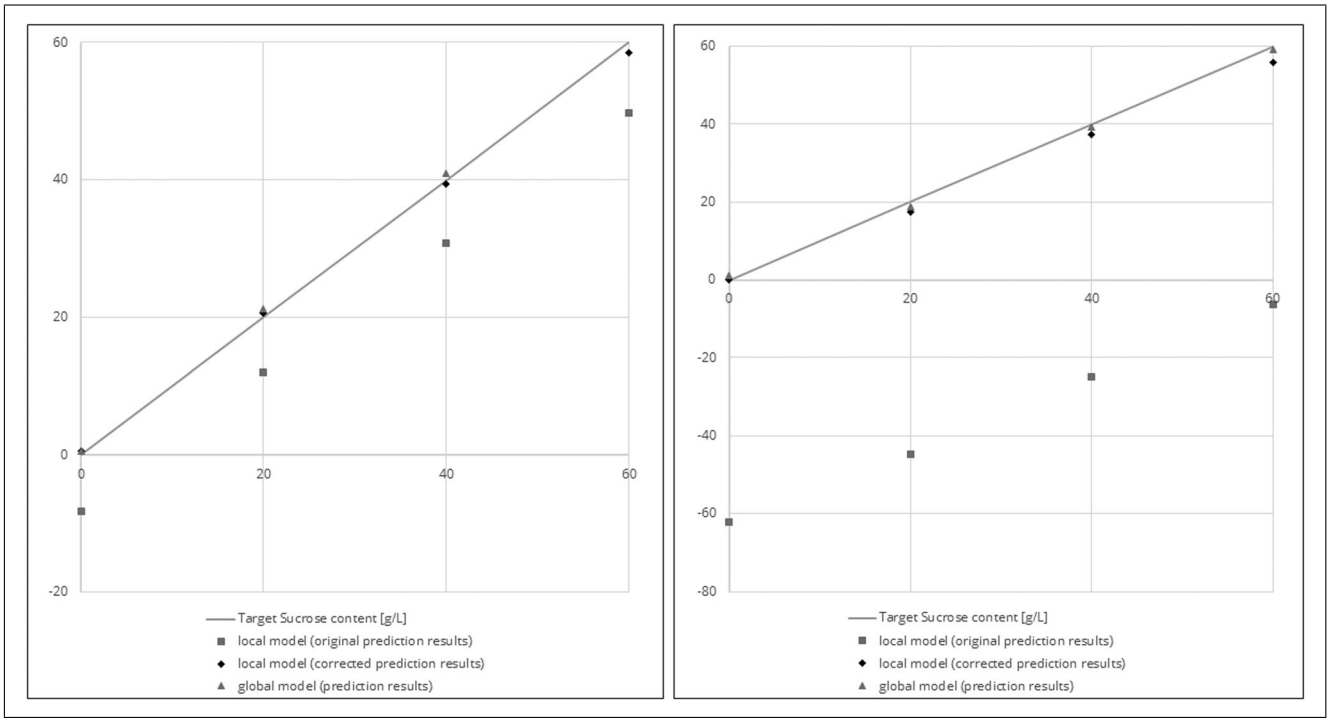

Figure 6–Prediction results for the sugar concentration of local model before and after correction via RMSEP regression equation and of the comparison with global model; for the examples of the measuring temperature of 40 (left) and 80°C (right) in g/L with the target sugar content as diagonal.

liter for the RMSEP and °C for the temperature. The regression statistics show with a *F*-value much higher than the significance *F*-value that there is a significant correlation between the dependent and independent variable, that is, that there is at least one non-zero regression coefficient. Results of the statistical evaluation were shown in Table 14. The *t*-test was used to check which of the regression coefficients are not equal to zero and whether they are statistically validated at a significance level of 5%. All regression coefficients show a value of *t Stat* unequal to zero and also have *p*-values smaller than .05, thus proving their significance. Using this equation, the correction values for prediction results of the two test set temperatures of 40 and 80 °C were calculated. The RMSEP value for 40 and 80 °C was 8.699 and 62.275 g/L, respectively. Calculation of the summed deviations from predicted to target sugar content of the two methods for the two measurement temperature of 40 and 80 °C as examples showed little differences in trueness (shown in Figure 6, left, for the temperature of 40 °C and in Figure 6, right, for 80 °C). The application of the method thus proved to be successful.

3.7 Comparison of the two compensation methods for temperature influence

A comparison of both methods was done to verify which one performs better in this kind of application. This was done by summing up the deviations of predicted sugar concentration from target concentration, considering the two measuring temperatures 40 and 80 °C. For the measuring temperature of 40 °C, the sum of deviation was 3.209 g/L when predicted and corrected with the local model and 3.892 g/L when predicted with the global model. For the 80 °C measurements, the sum of deviation for local corrected model and global model was 9.161

and 3.656 g/L, respectively. Comparing the corrected prediction results of the local model with the results reached with the global model, it can be seen that both methods perform successfully, whereas method of global model leads to slightly better results in terms of trueness. Which method should be chosen for other applications depends on the process itself, the measurement conditions, and the time frame for calibration. Basically, the method using a regression of the RMSEP is more complex in the post-treatment of the data and is only worthwhile if it is not possible or is only associated with a much higher expenditure of time to generate the calibration data, that is, to carry out a corresponding number of measurements at different temperatures. Furthermore, the danger of undiscovered errors creeping in during the application of chemometric methods and further processing steps of raw spectra into regression model is higher than the identification of faulty process control. In later work, the method of RMSEP regression should be verified using more complex systems or real beverages.

4. CONCLUSIONS

The results indicate that the flow rate or Reynolds number has in the tested range no relevant influence on robustness or reproducibility of measurement and on trueness in the meaning of multivariate data analysis. In contrast, the temperature was identified as an influencing parameter. While the robustness of the measurements increased with increasing temperature, the trueness of the multivariate data analysis decreased simultaneously due to a reduced variance within the calibration data. Considering this, two strategies of correction methods were tested and compared. Both strategies of correction led to comparable and tolerable error values, the former involving more workload during the experimental procedure and the latter during data processing. A further outcome was that a smaller path length leads to a higher accuracy. Hence, a narrower path length is preferable for the application of the transfection probe to quantify sugar concentration in a water–sugar solution. With identification of a relevant process parameter and setting as well as the establishment of a compensation strategy, the applicability for using near infrared spectroscopy as process analytical tool within a continuous flash pasteurization system is proven.

ACKNOWLEDGMENT

The Polytec GmbH (Waldbronn, Germany) is acknowledged for the loan of the spectrometer. The project SMARTPas (13FH024IX6) is financial supported by the Federal Ministry of Education and Research (BMBF).

AUTHOR CONTRIBUTIONS

I.W. conceived and designed the study and was in charge of overall direction and planning with input of J.S. I.W. performed the measurements. I.W. and M.Z. processed the experimental data and performed the analysis. P.N., J.S., and I.W. were involved in the interpretation of the results and I.W. wrote the manuscript with input from all authors.

REFERENCES

Adams, M. J. (2004). *Chemometrics in analytical spectroscopy* (2. ed.). RSC analytical spectroscopy monographs: Vol. 8. Cambridge: Royal Society of Chemistry.

Arimoto, H., Tarumi, M., & Yamada, Y. (2003). Temperature-insensitive measurement of glucose concentration based on near infrared spectroscopy and partial least squares analysis. *Optical Review*, *10*(2), 74–76. https://doi.org/10.1007/s10043-003-0074-z

Blanco, M., & Romero, M. A. (2001). Near-infrared libraries in the pharmaceutical industry: A solution for identity confirmation. *The Analyst*, *126*(12), 2212–2217. https://doi.org/10.1039/B105012P

Bock, J. E., & Connelly, R. K. (2008). Innovative uses of near-infrared spectroscopy in food processing. *Journal of Food Science*, *73*(7), R91-8. https://doi.org/10.1111/j.1750-3841.2008.00870.x

Büning-Pfaue, H. (2003). Analysis of water in food by near infrared spectroscopy. *Food Chemistry*, *82*(1), 107–115. https://doi.org/10.1016/S0308-8146(02)00583-6

Burns, D. A., & Ciurczak, E. W. (2008). *Handbook of near-infrared analysis* (3rd ed.). Practical spectroscopy: Vol. 35. Boca Raton, FL: CRC Press.

Cen, H., Bao, Y., & He, Y., Sun, D. W. (2007). Visible and near infrared spectroscopy for rapid detection of citric and tartaric acids in orange juice. *Journal of Food Engineering*, *82*(2), 253–260. https://doi.org/10.1016/j.jfoodeng.2007.02.039

Cen, H., & He, Y. (2007). Theory and application of near infrared reflectance spectroscopy in determination of food quality. *Trends in Food Science & Technology*, *18*(2), 72–83. https://doi.org/10.1016/j.tifs.2006.09.003

Chen, T., & Martin, E. (2007). The impact of temperature variations on spectroscopic calibration modelling: A comparative study. *Journal of Chemometrics*, *21*(5-6), 198–207. https://doi.org/10.1002/cem.1041

Cozzolino, D., Cynkar, W. U., Shah, N., & Smith, P. (2011). Multivariate data analysis applied to spectroscopy: Potential application to juice and fruit quality. *Food Research International*, *44*(7), 1888–1896. https://doi.org/10.1016/j.foodres.2011.01.041

Cozzolino, D., Liu, L., Cynkar, W. U., Dambergs, R. G., Janik, L., Colby, C. B., & Gishen, M. (2007). Effect of temperature variation on the visible and near infrared spectra of wine and the consequences on the partial least square calibrations developed to measure chemical composition. *Analytica Chimica Acta*, *588*(2), pp. 224–230.

Cozzolino, D., Parker, M., Dambergs, R. G., Herderich, M., & Gishen, M. (2006). Chemometrics and visible-near infrared spectroscopic monitoring of red wine fermentation in a pilot scale. *Biotechnology and Bioengineering*, *95*(6), 1101–1107. https://doi.org/10.1002/bit.21067

Dammann, A., Schwarzer, K., Müller, U., & Schneider, J. (2011). Flash pasteurization of beer – a critical review. *Brewing Science*, *64*, 32–40.

Dammann, A., Schwarzer, K., Müller, U., & Schneider, J. (2014). Evaluation of the acidic sucrose hydrolysis as time-temperature integrator in flash pasteurizers. *Brewing Science*, *67*, 10–17.

Dammann, A., Schwarzer, K., Neubauer, P., & Schneider, J. (2014). Effect of residence time distribution in flash pasteurizers on the thermal death of microorganisms. *Brewing Science*, *67*, 101–107.

Dammann, A., Schwarzer, K., Vullriede, T., Müller, U., & Schneider, J. (2012). Determination of the kinetic parameters of a time-temperature integrator for the flash pasteurization. *Brewing Science*, *65*, 130–135.

Debebe, A., Temesgen, S., Abshiro, M. R., & Chandravanshi, B. S. (2017). Partial least squares–near infrared spectrometric determination of ethanol in distilled alcoholic beverages. *Bulletin of the Chemical Society of Ethiopia*, *31*(2), 201. https://doi.org/10.4314/bcse.v31i2.2

Dialekt Projekt (2002). *Statistik interaktiv! Deskriptive Statistik* (2nd ed.). Berlin, Heidelberg: Springer Berlin Heidelberg.

Gallignani, M., Garrigues, S., & de la Guardia, M. (1993). Direct determination of ethanol in all types of alcoholic beverages by near-infrared derivative spectrometry. *The Analyst*, *118*(9), 1167. https://doi.org/10.1039/AN9931801167

Golic, M., Walsh, K., & Lawson, P. (2003). Short-wavelength near-infrared spectra of sucrose, glucose, and fructose with respect to sugar concentration and temperature. *Applied Spectroscopy*, *57*(2), 139–145. https://doi.org/10.1366/000370203321535033

Grassi, S., & Alamprese, C. (2018). Advances in NIR spectroscopy applied to process analytical technology in food industries. *Current Opinion in Food Science*, *22*, 17–21. https://doi.org/10.1016/j.cofs.2017.12.008

Hageman, J. A., Westerhuis, J. A., & Smilde, A. K. (2017). Temperature robust multivariate calibration: an overview of methods for dealing with temperature influences on near infrared spectra. *Journal of Near Infrared Spectroscopy*, *13*(2), 53–62. https://doi.org/10.1255/jnirs.457

Halsey, S. A. (1985). The use of transmission and transflectance near infrared spectroscopy for the analysis of beer. *Journal of the Institute of Brewing*, *91*(5), 306–312. https://doi.org/10.1002/j.2050-0416.1985.tb04348.x

Hitzmann, B., Hauselmann, R., Niemoeller, A., Sangi, D., Traenkle, J., & Glassey, J. (2015). Process analytical technologies in food industry - challenges and benefits: A status report and recommendations. *Biotechnology Journal*, *10*(8), 1095–1100. https://doi.org/10.1002/biot.201400773

Huang, H., Yu, H., Xu, H., & Ying, Y. (2008). Near infrared spectroscopy for on/in-line monitoring of quality in foods and beverages: A review. *Journal of Food Engineering*, *87*(3), 303–313. https://doi.org/10.1016/j.jfoodeng.2007.12.022

Kähler, W. M. (2010). Statistische Datenanalyse: Verfahren verstehen und mit SPSS gekonnt einsetzen; [mit Online-Service] (6., verb. u. erw. Aufl.). Studium.

Kessler, W. (2007). *Multivariate Datenanalyse: für die Pharma-, Bio- und Prozessanalytik (1., Auflage, neue Ausgabe)*. Weinheim: Wiley-VCH.

Kümmel, W. (2004). *Technische Strömungsmechanik: Theorie und Praxis (2., durchgesehene und korrigierte Auflage)*. Wiesbaden: Vieweg+Teubner.

Lachenmeier, D. W., Godelmann, R., Steiner, M., Ansay, B., Weigel, J., & Krieg, G. (2010). Rapid and mobile determination of alcoholic strength in wine, beer and spirits using a flow-through infrared sensor. *Chemistry Central Journal*, *4*, 5. https://doi.org/10.1186/1752-153X-4-5

Lanza, E., & Li, B. W. (1984). Application for near infrared spectroscopy for predicting the sugar content of fruit juices. *Journal of food science*, *49*(4), 995–998. https://doi.org/10.1111/j.1365-2621.1984.tb10378.x

Lewis, M. J., & Heppell, N. J. (2012). *Continuous thermal processing of foods: Pasteurization and UHT sterilization*. U.S.A.: Kluwer Academic.

OMVE Netherlands B.V. (2018). HT220 Laboratory Heat Treatment System: Inline Pasteurization and Sterilization. Retrieved from https://omve.com/product/ht220-series-lab-uht-htst-system/

Osborne, B. G. (2006). Near-infrared spectroscopy in food analysis. In R. A. Meyers, & R. J. McGorrin (Eds.), *Encyclopedia of analytical chemistry*. New York: John Wiley & Sons, Ltd. https://doi.org/10.1002/9780470027318.a1018

Porep, J. U., Kammerer, D. R., & Carle, R. (2015). On-line application of near infrared (NIR) spectroscopy in food production. *Trends in Food Science & Technology*, *46*(2), 211–230. https://doi.org/10.1016/j.tifs.2015.10.002

Schmidt, T. (2000). *Viskositäts- und Oberflächenspannungsverhalten von reinen und technischen Saccharoselösungen (Dissertation)*. Technische Universität Berlin, Berlin.

Spurk, J. H. (1987). *Strömungslehre: einführung in die Theorie der Strömungen*. Berlin, Heidelberg: Springer Berlin Heidelberg.

Swierenga, H., Wülfert, F., de Noord, O. E., de Weijer, A. P., Smilde, A. K., & Buydensa, L. M. C. (2000). Development of robust calibration models in near infra-red spectrometric applications. *Analytica Chimica Acta*, *411*(1-2), pp. 121–135.

Swindells, J. F., Snyder, C. F., Hardy, R. C., & Golden, P. E. (1958). *Viscosities of sucrose solutions at various temperatures: tables of recalculated values*. Washington: U.S. Government Printing Office.

Van den Berg, F., Lyndgaard, C. B., Sørensen, K. M., & Engelsen, S. B. (2013). Process Analytical Technology in the food industry. *Trends in Food Science & Technology*, *31*(1), 27–35. https://doi.org/10.1016/j.tifs.2012.04.007